11-1995

# Heterodyne Ladar System Efficiency Enhancement Using Single-mode Optical Fiber Mixers

Donald K. Jacob
*University of Dayton*

Martin B. Mark
*Wright Laboratory*

Bradley D. Duncan
*University of Dayton*, bduncan1@udayton.edu

# Heterodyne ladar system efficiency enhancement using single-mode optical fiber mixers

**Donald K. Jacob**
University of Dayton
Center for Electro-Optics
300 College Park
Dayton, Ohio 45469-0245

**Martin B. Mark,** MEMBER SPIE
Wright Laboratory
AARI-2, Electro-Optics Sensors Group
Wright Patterson Air Force Base, Ohio 45433

**Bradley D. Duncan,** MEMBER SPIE
University of Dayton
Center for Electro-Optics
300 College Park
Dayton, Ohio 45469-0245

**Abstract.** A theoretical performance analysis of a heterodyne ladar system incorporating a single-mode fiber receiver has been performed. For our purposes, the performance parameters of interest are the coupling and mixing efficiency of the ladar receiver, as they relate to the overall system carrier-to-noise ratio. For a receiver incorporating a single-mode fiber mixer, the received and local-oscillator fields are matched both spatially and temporally at the detector, yielding 100% mixing efficiency. We have therefore focused our efforts on determining an expression for the efficiency with which a diffuse return from a purely speckle target can be coupled into the receiving leg of a monostatic, untruncated cw ladar system. Through numerical analysis, the expected coupling efficiency for a ladar system with negligible truncation of the transmit beam has been determined to be 30.6%.

*Subject terms: optical remote sensing and image processing; ladar; lidar; heterodyne; single-mode fibers; laser speckle.*

*Optical Engineering 34(11), 3122–3129 (November 1995).*

## 1 Introduction

Laser radar, LIDAR (light detection and ranging) or LADAR (laser detection and ranging) systems, the latter term being preferred, offer some advantages over conventional radar systems. These advantages are characteristic of the shorter-wavelength radiation emitted by the ladar source. For example, due to the ability to $Q$-switch lasers, extremely short pulse widths can be achieved and thus highly accurate range measurements are possible.[1] Also, because the angular divergence of a transmitted beam as it propagates in space is directly proportional to its wavelength, short-wavelength ladar systems are capable of making highly accurate angular measurements.[2]

Ladar does, however, have some disadvantages when compared to conventional radar. For example, microwave sources are much more power-efficient than ladar sources, the efficiency of a ladar source[3] (i.e., optical power out divided by electrical power in) ranging from less than 1% up to about 30%. Secondly, as the source wavelength gets shorter and approaches the size of atmospheric particles, a greater percentage of the transmitted power may be adversely affected by scattering and absorption.[4]

To accurately determine target information (range, velocity, shape, etc.) at long range and through a turbulent atmosphere, a ladar system must be able to detect weak signals. Often a coherent detection scheme (as opposed to a direct detection scheme) is used in applications where accurate range and velocity measurements are required because of the high receiver sensitivities that are obtainable. In a heterodyne receiver, the frequency of the signal returning from a distant target is compared with the frequency of a reference, or local-oscillator, signal on detection. The difference in frequency between the two signals is referred to as the intermediate frequency (IF); from it, the desired target information is then extracted. If the coherent receiver is operated so that the local-oscillator shot noise dominates over all other noises, near-quantum-limit receiver sensitivities are possible.[5]

A defining parameter for the performance of a ladar system is the system carrier-to-noise ratio (CNR). The CNR is the ratio of the signal power to the noise power, and is equivalent to the more commonly used signal-to-noise ratio (SNR) when the effects of fluctuations in received power due to target variations and atmospheric turbulence are neglected.[6] In a heterodyne detection scheme, the usable portion of the return signal (i.e., the portion of the return signal collected by the receiver aperture that contributes to the IF signal) is that portion of the received field that is of the same spatial and temporal mode as the local-oscillator field.[7] Increasing the percentage of the power collected by the receiver aperture that contributes to the IF signal power increases the system CNR and therefore the ability of the receiver to detect weak return signals. The performance of the ladar system can thus be characterized by a system efficiency. The system effi-

Paper RS-017 received Dec. 10, 1994; revised manuscript received June 9, 1995; accepted for publication June 19, 1995.

ciency is equivalent to the percentage of the received power that contributes to the IF signal power and can ideally be expressed as the product of the coupling efficiency (i.e., the percentage of the signal collected by the receiver aperture that is actually incident on the detector) and the mixing efficiency (i.e., the percentage of the received power incident on the detector that mixes with the local oscillator and contributes to the IF signal power). In actuality, the system efficiency will also include a factor representative of other optical losses in the system, such as splice and connector losses, as well as one that describes the efficiency of the detection process.

Traditionally, the mixing of the local-oscillator and return signal occurs in free space. This method of mixing results in a system efficiency of 25% for the worst-case scenario of a diffuse target in the far field and negligible truncation of Gaussian local-oscillator and transmit signals.[8,9] However, for free-space mixing Rye and Frehlich have reported[10] an optimum system efficiency of 43.8%. This result was obtained by truncating the local-oscillator and transmit beams so as to cause a higher spatial matching between the return signal and local-oscillator fields on the detector. (Note that the free-space system efficiency is equivalent to the mixing efficiency, because it is assumed that all the power collected by the receiver aperture is incident on the detector.) In real-world applications, though, a ladar system must first be robust. That is, it should be impervious to misalignment due to operator handling, environmental vibrations, etc. It should also be easily assembled and disassembled. It is for these reasons that many ladar systems currently employ single-mode fiber mixers.

For a mixer incorporating single-mode fibers, only the $LP_{01}$ mode is allowed. This results in ideal spatial matching between the received and local-oscillator fields on the detector, and thus 100% mixing efficiency. The other factor, however, that must be considered when dealing with a fiber mixing arrangement is the efficiency with which the return field is coupled into the allowed propagating mode of the single-mode fiber. We expect the coupling of a diffuse return (worst case) into the single propagating mode of the fiber to be somewhat limited. That is, the diffuse return contains many spatial frequencies, whereas the $LP_{01}$ mode can be characterized by a bandlimited set of spatial frequencies. Thus only those spatial frequencies of the return that correspond to those in the spatial-frequency spectrum of the $LP_{01}$ mode will be coupled into the receiving fiber. Ideally the system efficiency of the single-mode fiber mixer is equivalent to this coupling efficiency. We have therefore focused our efforts on determining an expression for the coupling efficiency of a diffuse return from a purely speckle target into the receiving leg of a monostatic, untruncated cw ladar system. In the analysis that follows we assume no depolarization of the diffuse return signal.

In Sec. 2, a *standard* form of the CNR applicable to any coherent mixing geometry is developed. In Sec. 3 we describe a general ladar system on which the subsequent theory is based. In order to limit the scope of this article, only our theoretical analysis will be presented here. An expression for the field received from a purely speckle target located in the far field and oriented normal to the ladar transmit-receive axis is then developed in Sec. 4. In Sec. 5 we then develop an expression for the efficiency with which this field couples to the return leg of the single-mode fiber mixer. Optimization of the coupling efficiency is then discussed in Sec. 6, followed by our conclusions in Sec. 7.

## 2 System Efficiency and the Shot-Noise Limited CNR

The CNR can be used as a defining performance parameter for a ladar system. The CNR for a coherent system is the ratio of the IF electronic signal power to the IF electronic noise power. We will write the CNR in a *standard* form applicable to any coherent system and discuss what will be referred to as the system efficiency. The system efficiency will be shown to be dependent on the detection process and how efficiently the power received from a target is utilized.

To determine a system CNR we must first determine an expression for the IF electronic signal power. The first stage of the detection process utilizes a photodetector, which responds to some incident radiation. For a coherent system the photodetector responds to the sum of the local-oscillator and return signal fields. The output current of the detector is then equal to the product of the detector responsivity $\Re$ and the intensity of the field distribution on the detector. After filtering at the intermediate frequency, and assuming monochromatic fields of the same spatial mode, we can represent the ideal IF output current from the detector as

$$i_{\mathrm{IF}}(t)=2\Re(P_{\mathrm{LO}}P_{RX})^{1/2}\cos(2\pi\nu_{\mathrm{IF}}t)\ , \tag{1}$$

while the IF signal power is

$$P_{\mathrm{IF}}=\langle i_{\mathrm{IF}}^2\rangle=2\Re^2P_{\mathrm{LO}}P_{\mathrm{RX}}\ , \tag{2}$$

where $P_{\mathrm{LO}}$ is the local oscillator power, $P_{\mathrm{RX}}$ is the return power, $\Re$ is the responsivity of the detector, and $\nu_{\mathrm{IF}}$ is the intermediate frequency.

The IF electronic noise current is equal to the superposition of the several noise sources inherent to the detection process. The primary noise sources of concern are well documented and are referred to as, for example, shot or quantum noise, thermal or Johnson noise, and dark-current noise.[3,11,12] The generation of these noise terms is a random process, and they are therefore discussed in terms of the mean squared noise current values, which are equivalent to noise powers assuming a 1-$\Omega$ load resistance. The total mean squared noise current $i_n^2$ is then given by

$$\langle i_n^2\rangle=2q\Re B(P_{\mathrm{LO}}+P_{\mathrm{RX}})+\frac{4k_BTB}{R_{\mathrm{load}}}+2qBI_d\ , \tag{3}$$

where, from left to right, the three terms on the right-hand side represent shot, thermal, and dark-current noise, and where $q$ is the electron charge, $B$ is the receiver bandwidth, which we assume is matched to the signal bandwidth, $k_B$ is Boltzman's constant, $T$ is the temperature in Kelvins, $I_d$ is the dark current produced by the detector, and $R_{\mathrm{load}}$ is the load resistance. An amplifier with gain $G$ is also usually required to boost the IF signal power above the noise level of the device being used to measure the signal. Thus the CNR can be written as

$$\mathrm{CNR} = \frac{2G\Re^2 P_{\mathrm{LO}} P_{\mathrm{RX}}}{G(2q\Re BP_{\mathrm{LO}} + 2q\Re BP_{\mathrm{RX}} + 4k_B TB/R_{\mathrm{load}} + 2qBI_d) + \Gamma_{\mathrm{amp}}}, \tag{4}$$

where $\Gamma_{\mathrm{amp}}$ is the noise power introduced by the amplifier.

Next we rewrite the CNR in a *standard* form, which can be used to describe the efficiency of the detection process. Specifically, we can factor out the local-oscillator shot-noise component of Eq. (4) to obtain

$$\mathrm{CNR} = \frac{\Re}{qB} P_{\mathrm{RX}} \left( 1 + \frac{P_{\mathrm{RX}}}{P_{\mathrm{LO}}} + \frac{2k_B T}{q\Re P_{\mathrm{LO}} R_{\mathrm{load}}} + \frac{I_d}{\Re P_{\mathrm{LO}}} + \frac{\Gamma_{\mathrm{amp}}}{2qG\Re BP_{\mathrm{LO}}} \right)^{-1}, \tag{5}$$

or

$$\mathrm{CNR} = \frac{\eta}{h\nu B} P_{\mathrm{RX}} \eta_{\mathrm{det}}, \tag{6}$$

where the responsivity of the detector has been written out explicitly (i.e., $\Re = \eta q/h\upsilon$, where $\eta$ is the quantum efficiency of the photodetector, $h$ is Planck's constant, and $\upsilon$ is the optical frequency) and the bracketed terms of Eq. (5), which we will call the detection efficiency, are grouped into $\eta_{\mathrm{det}}$ in Eq. (6). When the local oscillator power is adjusted so that the last four terms in the detection efficiency are negligible (i.e., $\eta_{\mathrm{det}} \approx 1$), the detection process is referred to as shot-noise-limited and EQ. (6) is referred to as the shot-noise-limited CNR. Note that in the previous analysis only the most common noise factors were included. Of course, there are several other potential noise terms that we have not included, but all would result in terms having the same general form as those bracketed in Eq. (5). That is, by adjusting the local-oscillator power, $\eta_{\mathrm{det}}$ can always be made to be approximately equal to one.

Realistically, the return signal from the target will contain many spatial modes, due either to variations in the target or to atmospheric turbulence. Therefore, even under the condition of shot-noise-limited detection, there are still other factors that affect the efficiency with which the total received power is utilized in the detection process. Primarily these factors are the coupling and mixing efficiencies mentioned previously. Considering these efficiency factors now, the optimum (i.e., no optical loss after reception) shot-noise-limited CNR can be expressed in standard form as

$$\mathrm{CNR} = \frac{\eta}{h\nu B} P_{\mathrm{RX}} \eta_m \eta_c = \frac{\eta}{h\nu B} P_{\mathrm{RX}} \eta_s = \frac{\eta}{h\nu B} P_{\mathrm{sig}}, \tag{7}$$

where $\eta_s$ is the overall system efficiency (i.e., the percentage of the received power that contributes to the IF signal power), $\eta_c$ is the coupling efficiency, $\eta_m$ is the mixing efficiency, and $P_{\mathrm{sig}}$ is the optical power contributing to the IF return signal. Note that had we not assumed shot-noise-limited detection, the detection efficiency $\eta_{\mathrm{det}}$ from Eq. (6) would have also been included in the system efficiency.

To reiterate, though Eq. (7) is general, for the single-mode fiber mixer all of the power coupled into the receiver leg of the mixer can ideally be made to contribute to the IF signal power. Therefore, assuming all optical losses are minimal, the efficiency of the single-mode fiber mixer depends primarily on the efficiency with which the power received from the target couples to the single propagating mode of the fiber. The remainder of this paper investigates this efficiency.

## 3 General Ladar System

Figure 1 is a diagram of an idealized monostatic cw ladar system on which the theory of Sec. 4 is based. The ladar source emits a monochromatic, Gaussian beam, which passes through an optical isolator used to prevent the source radiation from reentering the laser. A portion of the beam is directed to the acousto-optic modulator (AOM) by an *LO splitter*. The LO splitter consists of a polarizing beamsplitter cube (PBS) and a halfwave plate. Adjusting the halfwave plate adjusts the polarization angle of the source beam and allows variation of the local oscillator (LO) and transmit powers. After passing through the AOM, the LO beam is upshifted in frequency by an amount equal to the intermediate frequency $\nu_{\mathrm{IF}}$. This power is then coupled into the LO leg of the waveguide mixer by lens L1. The portion of the power not split off into the LO is expanded and collimated by the lens combination L2 and L3 and transmitted to the target, at a range $L$ assumed to be in the far field. The clear aperture of lens L3 defines the transmit-receive aperture and is located in the plane where the waist of the transmit beam is measured.

In the process of being expanded, the transmit beam passes through a transmit-receive switch consisting of an additional polarizing beamsplitter cube (PBS) and a quarterwave plate. The linear output of the source is thus converted to circular polarization before it is transmitted to the target. After reflecting off the target, the return energy remains primarily circularly polarized, but with opposite handedness to the transmitted beam. At the receiver aperture (diameter $d_R$), a portion of the energy reflected by the target is collected, after which it then passes back through the quarterwave plate and becomes linearly polarized orthogonal to the source polarization. It is then directed towards the return leg of the waveguide mixer by the polarizing beamsplitter cube and lenses L3 and L4. (Note that we are assuming the target does not depolarize the incident beam. If it did, an additional loss term would be included in the overall system efficiency, representing the portion of the return that is lost to depolarization). As for the optical waveguide mixer, although only one of the

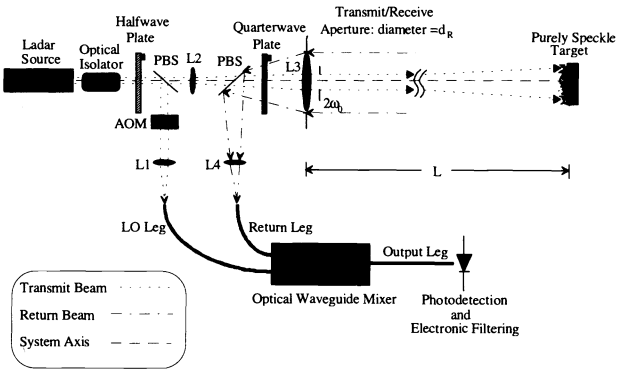


**Fig. 1** The general ladar system on which the theory for the fiber mixer is based.

two possible output legs of the assumed evanescent wave coupler-mixer is shown, both outputs can in general be used via a balanced mixing arrangement. We have shown one output leg for simplicity only. For this system, then, the limiting parameter of interest is the efficiency with which the diffuse return couples into the return leg of the optical mixer.

## 4 Received Field

Before determining the coupling efficiency, we must first determine an expression for the field received from the speckle target that is focused onto the single-mode fiber end face. For this analysis we assume a resolved, stationary speckle target located in the far field, oriented normal to the transmit-receive axis. We also assume the detection process is LO shot-noise-limited. For the notation, an underscore indicates a complex quantity, boldface indicates a vector quantity, and a tilde indicates a random quantity.

To determine an expression for the received field, we propagate the transmitted field $U_{\mathrm{TX}}$ (referred to the transmitter aperture) to the target, using the free-space Green's function, and multiply by the target's complex reflection coefficient $\tilde{T}(\boldsymbol{\rho}_t)$. We then back-propagate the resulting field to the receiver aperture, using the same Green's function, and then through the receiving optics to the focal plane. Note that the return fiber is assumed to be located in the focal plane of the receiver optics and centered for maximum coupling. This will thus give us the field on the end face of the fiber, $\tilde{U}_f(\boldsymbol{\rho}_f)$, in terms of the target and system characteristics.

Assuming receiver optics focal lengths on the order of tens of centimeters and waveguide core diameters on the order of a few wavelengths, the received field, after neglecting terms that are insignificant in the far field, can be written as

$$\tilde{U}_f(\boldsymbol{\rho}_f)=\frac{1}{(j\lambda f)(\lambda L)^2}\iint_{\infty} d\boldsymbol{\rho}_R\ W_R(\boldsymbol{\rho}_R)\ \exp\left(-\frac{jk}{f}\boldsymbol{\rho}_f\cdot\boldsymbol{\rho}_R\right)$$
$$\times\iint_{A_t} d\boldsymbol{\rho}_t\ \tilde{T}(\boldsymbol{\rho}_t)\ \exp\left(\frac{jk}{L}\boldsymbol{\rho}_t\cdot\boldsymbol{\rho}_R\right)$$
$$\times\iint_{A_T} d\boldsymbol{\rho}\ U_{\mathrm{TX}}(\boldsymbol{\rho})\ \exp\left(-\frac{jk}{L}\boldsymbol{\rho}\cdot\boldsymbol{\rho}_t\right)\ , \tag{8}$$

where $\lambda$, $f$, and $L$ are the source wavelength, receiver optics focal length, and target range, respectively, and $k=2\pi/\lambda$ is the free-space wave number. The two-dimensional spatial variables $\boldsymbol{\rho}_R$, $\boldsymbol{\rho}_t$, and $\boldsymbol{\rho}$ represent the receiver, target, and transmit aperture planes, respectively, and $\boldsymbol{\rho}_f$ is the two-dimensional spatial variable representing the focal plane of the receiver optics. Furthermore, $W_R$ is the receiver aperture function, and $A_t$ and $A_T$ are the target and transmit aperture areas, respectively. Equation (8) is now seen to be a sequence of Fourier transform integrals. Reading Eq. (8) from right to left, we see that the transmitted beam is first Fourier-transformed to the far field, where it is then multiplied by the complex reflection coefficient of the target and Fourier-transformed back to the receiver aperture. In this plane the field is truncated (multiplied) by the receiver aperture function, after which it is finally Fourier-transformed to the focal plane of the coupling optics.

The expression for the field at the focal plane of the coupling optics, as given in Eq. (8), is written in a very appealing form, but with some rearranging can be written more compactly. Thus we obtain

$$\tilde{U}_f(\boldsymbol{\rho}_f)=\frac{1}{(j\lambda f)(\lambda L)^2}\iint_{A_t} d\boldsymbol{\rho}_t\ \tilde{T}(\boldsymbol{\rho}_t)$$
$$\times\iint_{A_T} d\boldsymbol{\rho}\ U_{\mathrm{TX}}(\boldsymbol{\rho})\ \exp\left(-\frac{jk}{L}\boldsymbol{\rho}\cdot\boldsymbol{\rho}_t\right)$$
$$\times\iint_{\infty} d\boldsymbol{\rho}_R\ W_R(\boldsymbol{\rho}_R)\ \exp\left[-j2\pi\boldsymbol{\rho}_R\cdot\left(\frac{\boldsymbol{\rho}_f}{\lambda f}-\frac{\boldsymbol{\rho}_t}{\lambda L}\right)\right]\ . \tag{9}$$

Now, making the assumption of negligible truncation of the transmitted beam at the transmitting aperture, the limits on the $\boldsymbol{\rho}$ integral can be extended to the entire plane and Eq. (9) can be written in terms of Fourier transform as

$$\tilde{U}_f(\boldsymbol{\rho}_f)=$$
$$\frac{1}{(j\lambda f)(\lambda L)^2}\iint_{A_t} d\boldsymbol{\rho}_t\ \tilde{T}(\boldsymbol{\rho}_t)\ \mathcal{U}_{\mathrm{TX}}\left(\frac{\boldsymbol{\rho}_t}{\lambda L}\right)\mathcal{W}_R\left(\frac{\boldsymbol{\rho}_f}{\lambda f}-\frac{\boldsymbol{\rho}_t}{\lambda L}\right)\ , \tag{10}$$

where $\mathcal{U}_{\mathrm{TX}}$ is the Fourier transform of the transmit beam and $\mathcal{W}_R$ is the Fourier transform of the receiver aperture function. Equation (10) represents in essence the image of the target in the focal plane of the lens, with illumination given by the far-field pattern of the transmitted beam, and with the image blurred by the diffraction introduced by the Fourier transform of the receiver aperture.

## 5 Single-Mode Fiber Coupling Efficiency

A single-mode fiber will only support the propagation of the $\mathrm{LP}_{01}$ mode. For a single-mode fiber mixing scheme, the LO and the received optical fields propagating in their respective legs of the fiber mixer will thus be identical. We normalize this field pattern to unit power and designate it as $U_{01}(\boldsymbol{\rho}_f)$. Summing the fields on the photodetector and taking the squared magnitude, the positive-frequency IF signal portion of the photodetector output is, in phasor notation,

$$\tilde{y}(t)=$$
$$\frac{q\eta}{h\nu}\iint_{A_d} d\boldsymbol{\rho}_f\ [\tilde{P}_{\mathrm{sig}}^{1/2}U_{01}^{*}(\boldsymbol{\rho}_f)][P_{\mathrm{LO}}^{1/2}U_{01}(\boldsymbol{\rho}_f)\ \exp(j2\pi\nu_{\mathrm{IF}})]\ , \tag{11}$$

where $\tilde{P}_{\mathrm{sig}}$ is the received optical power coupled into and propagating in the fiber, and $A_d$ is the detector area, assumed to be much larger than the field extent. Notice also that because of the diffuse nature of the target, $\tilde{P}_{\mathrm{sig}}$ and $\tilde{y}(t)$ are random variables.

Now, because $U_{01}$ is assumed to be normalized to unit power, the positive-frequency IF signal current out of the detector can be written as

$$\tilde{y}(t)=\frac{q\eta}{h\nu}(P_{\mathrm{LO}}\tilde{P}_{\mathrm{sig}})^{1/2}\exp(j2\pi\nu_{\mathrm{IF}}t)\ . \tag{12}$$

The expected time-average IF signal power $P_{\mathrm{IF}}$ is thus

$$P_{\mathrm{IF}}=\langle E[|\tilde{y}(t)|^2]\rangle=\left(\frac{q\eta}{h\nu}\right)^2 P_{\mathrm{LO}}E[\tilde{P}_{\mathrm{sig}}]\ , \tag{13}$$

where the $E[\ ]$ indicates the statistical expectation of the quantity in brackets and $\langle\ \rangle$ indicates time averaging. Dividing the IF signal power by the expected LO shot-noise power ($q\Re BP_{\mathrm{LO}}$), the average CNR for the single-mode fiber mixer is, in standard form,

$$\mathrm{CNR}_{\mathrm{S.M.fiber}}=\frac{\eta}{h\nu B}E[\tilde{P}_{\mathrm{sig}}]\ . \tag{14}$$

Note that because we are using the phasor notation here, we are in actuality only looking at half the IF signal power, thus requiring the LO shot-noise term of Eq. (3) to be reduced by half. Ideally, all of the received power coupled into the fiber contributes to the expected time-average IF signal power. It now only remains to compute the power coupled to the fiber $E[\tilde{P}_{\mathrm{sig}}]$ in terms of the average power collected by the receiver aperture.

The power coupled into the fundamental fiber mode can be approximated[13] by using an overlap integral of the field focused on the end face of the fiber, $\tilde{U}_f(\boldsymbol{\rho}_f)$, and the complex conjugate of the normalized $\mathrm{LP}_{01}$ modal field, $U_{01}^*(\boldsymbol{\rho}_f)$:

$$\tilde{P}_{\mathrm{sig}}\approx\left|\iint \mathrm{d}\boldsymbol{\rho}_f\ \tilde{U}_f(\boldsymbol{\rho}_f)U_{01}^*(\boldsymbol{\rho}_f)\right|^2\ . \tag{15}$$

Substituting $\tilde{U}_f(\boldsymbol{\rho}_f)$ from Eq. (10) into Eq. (15) and rearranging terms then yields

$$\tilde{P}_{\mathrm{sig}}\approx\left|\frac{1}{(j\lambda f)(\lambda L)^2}\iint_{A_t}\mathrm{d}\boldsymbol{\rho}_t\ \tilde{T}(\boldsymbol{\rho}_t)\mathcal{U}_{\mathrm{TX}}\left(\frac{\boldsymbol{\rho}_t}{\lambda L}\right)\right.$$
$$\left.\times\iint \mathrm{d}\boldsymbol{\rho}_f\ U_{01}^*(\boldsymbol{\rho}_f)\mathcal{W}_R\left(\frac{\boldsymbol{\rho}_f}{\lambda f}-\frac{\boldsymbol{\rho}_t}{\lambda L}\right)\right|^2\ . \tag{16}$$

We can now determine the expected power coupled into the single-mode fiber by taking the expectation of Eq. (16).

In finding the expected value of Eq. (16) we use the following statistical relationships for a purely speckle target[6]:

$$E[\tilde{T}(\boldsymbol{\rho}_{t1})]=0\ ,$$

$$E[\tilde{T}(\boldsymbol{\rho}_{t1})\tilde{T}(\boldsymbol{\rho}_{t2})]=0\ ,$$

$$E[\tilde{T}(\boldsymbol{\rho}_{t1})\tilde{T}^*(\boldsymbol{\rho}_{t2})]=\lambda^2T_0(\boldsymbol{\rho}_{t1})\delta(\boldsymbol{\rho}_{t1}-\boldsymbol{\rho}_{t2})\ , \tag{17}$$

where $E[\ ]$ indicates the statistical expectation, or ensemble average, of the quantity in brackets. Also in Eq. (17), $T_0(\boldsymbol{\rho}_{t1})$ is the average bidirectional reflectance per steradian, related to the diffuse reflectivity $\tau(\boldsymbol{\rho}_{t1})$ (a spatially dependent unitless number, ranging from 0 to 1) by[14]

$$T_0(\boldsymbol{\rho}_{t1})=\frac{\tau(\boldsymbol{\rho}_{t1})}{\pi}\ . \tag{18}$$

Note that if the target reflectivity is constant over the area of the target, Eq. (18) will be independent of the 2-D spatial coordinate $\boldsymbol{\rho}_{t1}$. We make this assumption in the analysis that follows. Thus, using Eqs. (16) and (17), the expected power coupled into the single-mode fiber can, after some manipulation, be written as

$$E[\tilde{P}_{\mathrm{sig}}]\approx\frac{T_0}{f^2(\lambda L)^4}\iint_{A_t}\mathrm{d}\boldsymbol{\rho}_t\ \left|\mathcal{U}_{\mathrm{TX}}\left(\frac{\boldsymbol{\rho}_t}{\lambda \mathrm{L}}\right)\right|^2$$
$$\times\iint \mathrm{d}\boldsymbol{\rho}_R\ W_R(\boldsymbol{\rho}_R)\mathcal{U}_{01}^*\left(-\frac{\boldsymbol{\rho}_R}{\lambda f}\right)\exp\left(j2\pi\boldsymbol{\rho}_R\cdot\frac{\boldsymbol{\rho}_t}{\lambda L}\right)$$
$$\times\iint \mathrm{d}\boldsymbol{\rho}'_R\ W_R^*(\boldsymbol{\rho}'_R)\mathcal{U}_{01}\left(-\frac{\boldsymbol{\rho}'_R}{\lambda f}\right)\exp\left(-j2\pi\boldsymbol{\rho}'_R\cdot\frac{\boldsymbol{\rho}_t}{\lambda l}\right), \tag{19}$$

where $\boldsymbol{\rho}_R$ and $\boldsymbol{\rho}'_R$ are both dummy spatial variables in the receiver aperture plane and $\mathcal{U}_{01}$ is the Fourier transform of the fundamental fiber mode field. In order to simplify the integration required of Eq. (19) we now make the following change of variables[15,16]:

$$\boldsymbol{\rho}_0\equiv\frac{\boldsymbol{\rho}'_R+\boldsymbol{\rho}_R}{2}\quad\text{and}\quad\Delta\boldsymbol{\rho}\equiv\boldsymbol{\rho}'_R-\boldsymbol{\rho}_R$$
$$\Rightarrow\quad\iint \mathrm{d}\boldsymbol{\rho}_R\iint \mathrm{d}\boldsymbol{\rho}'_R=\iint \mathrm{d}\boldsymbol{\rho}_0\iint \mathrm{d}\Delta\boldsymbol{\rho}\ . \tag{20}$$

Equation (19) can now be written as

$$E[\tilde{P}_{\mathrm{sig}}]\approx\frac{T_0}{f^2(\lambda L)^4}\iint \mathrm{d}\Delta\boldsymbol{\rho}\ \mathcal{F}\left\{\left|\mathcal{U}_{\mathrm{TX}}\left(\frac{\boldsymbol{\rho}_t}{\lambda L}\right)\right|^2\right\}\Big|_{\Delta\boldsymbol{\rho}/\lambda L}$$
$$\times\iint \mathrm{d}\boldsymbol{\rho}_0\ W_R\left(\boldsymbol{\rho}_0-\frac{1}{2}\Delta\boldsymbol{\rho}\right)$$
$$\times\mathcal{U}_{01}^*\left(-\frac{\boldsymbol{\rho}_0}{\lambda F}+\frac{1}{2}\frac{\Delta\boldsymbol{\rho}}{\lambda f}\right)W_R^*\left(\boldsymbol{\rho}_0+\frac{1}{2}\Delta\boldsymbol{\rho}\right)$$
$$\times\mathcal{U}_{01}\left(-\frac{\boldsymbol{\rho}_0}{\lambda f}-\frac{1}{2}\frac{\Delta\boldsymbol{\rho}}{\lambda f}\right)\ , \tag{21}$$

where $\mathcal{F}\{\ \}$ indicates the Fourier transform operation, and the integral over the target plane has been absorbed into $\mathcal{F}[|\mathcal{U}_{\mathrm{TX}}|^2]$. This is now as far as the analysis can go without giving the field and aperture functions specific forms.

The field inside the fiber is that of the $\mathrm{LP}_{01}$ mode of a circularly symmetric step-index dielectric waveguide. Strictly speaking, the field distribution of this mode is proportional to $J_0(\rho)$, the zero-order Bessel function of the first kind, in the fiber core, and proportional to $K_0(\rho)$, the zero-order modified Bessel function of the second kind, in the fiber cladding. Marcuse has shown, however, that a Gaussian function can very accurately approximate the $\mathrm{LP}_{01}$ field distribution.[17] Therefore, the normalized single-mode field distribution will be taken approximately to be

$$U_{01}(\boldsymbol{\rho}_f)\approx\left(\frac{2}{\pi\omega^2}\right)^{1/2}\exp\left(-\frac{|\boldsymbol{\rho}_f|^2}{\omega^2}\right)\ , \tag{22}$$

where Marcuse has also shown that the optimum choice for the parameter $\omega$ is given empirically by the equation[17]

$$\omega \equiv r_c g_0(V) = r_c\left(0.65 + \frac{1.619}{V^{3/2}} + \frac{2.879}{V^6}\right) , \tag{23}$$

where $r_c$ is the fiber core radius, $V$ is the normalized frequency of the fiber [i.e., $V \equiv 2\pi r_c (n_1^2 - n_2^2)^{1/2}/\lambda = 2\pi r_c \, \mathrm{NA}/\lambda$], $n_1$ and $n_2$ are the core and cladding indices of refraction, respectively, and NA is the numerical aperture of the fiber.

Next, we define the aperture function $W_R$ as having a circular shape with diameter $d_R$; that is,

$$W_R(\boldsymbol{\rho}) = \mathrm{circ}\left(\frac{\boldsymbol{\rho}}{d_R}\right) \equiv \begin{cases} 1, & |\boldsymbol{\rho}| \leq d_R/2, \\ 0, & |\boldsymbol{\rho}| > d_R/2, \end{cases} \tag{24}$$

and let the transmitted field $U_{\mathrm{TX}}(\boldsymbol{\rho})$, normalized to the transmitted power $P_{\mathrm{TX}}$, be a Gaussian function of the form

$$U_{\mathrm{TX}}(\boldsymbol{\rho}) = \left(\frac{2P_{\mathrm{TX}}}{\pi\omega_0^2}\right)^{1/2} \exp\left(-\frac{|\boldsymbol{\rho}|^2}{\omega_0^2}\right) , \tag{25}$$

where again $\boldsymbol{\rho}$ is a 2-D coordinate representing the transmit plane, and $\omega_0$ is the $1/e^2$ beam waist of the transmit beam. After substituting Eqs. (22), (24), and (25) into Eq. (21), rearranging terms, and scaling all spatial variables by $d_R$, we find

$$\begin{aligned} E[\tilde{P}_{\mathrm{sig}}] \approx \frac{4T_0 P_{\mathrm{TX}} d_R^2}{\pi L^2} \cdot a^2 \iint \mathrm{d}\Delta\boldsymbol{\rho} \, \exp\left[-\left(\frac{1}{2}R^2 + a^2\right)|\Delta\boldsymbol{\rho}|^2\right] \\ \times \iint \mathrm{d}\boldsymbol{\rho}_0 \, \exp(-4a^2|\boldsymbol{\rho}_0|^2) \, \mathrm{circ}\left(\boldsymbol{\rho}_0 + \frac{1}{2}\Delta\boldsymbol{\rho}\right) \\ \times \mathrm{circ}\left(\boldsymbol{\rho}_0 - \frac{1}{2}\Delta\boldsymbol{\rho}\right) , \end{aligned} \tag{26}$$

where $R = d_R/\omega_0$ is referred to as the system truncation ratio, $\omega$ is defined in Eq. (23), and the parameter $a$ is defined as

$$a \equiv \frac{1}{\sqrt{2}} \frac{\pi\omega d_R}{\lambda f} . \tag{27}$$

This is a useful parameter because it appears repeatedly in the expression for $E[\tilde{P}_{\mathrm{sig}}]$ and is related to either the system optics $f$ number ($f/\#$) or numerical aperture $\mathrm{NA}_{\mathrm{optics}}$ (for small numerical apertures), in that

$$f/\# = \frac{f}{d_R} = \frac{1}{2\ \mathrm{NA}_{\mathrm{optics}}} . \tag{28}$$

As we see in the following section, these quantities can be used to determine the relationship between the coupling efficiency and the numerical apertures of the coupling optics and the single-mode fiber mixer.

Notice now that the two exponentials in Eq. (26) are Gaussian functions centered at the origins of the $\boldsymbol{\rho}_0$ and $\Delta\boldsymbol{\rho}$ planes. The circ functions, however, are unit-diameter circles centered at $\pm\,1/2\,\Delta\boldsymbol{\rho}$ in the $\boldsymbol{\rho}_0$ plane, and the $\boldsymbol{\rho}_0$ integral is therefore nonzero only when and where the two circ functions overlap. For instance, for $|\Delta\boldsymbol{\rho}| > 1$ the two circ functions will not overlap at all and the entire equation is identically equal to zero. Figure 2 depicts a graph of circ $(\boldsymbol{\rho}_0 + 1/2\Delta\boldsymbol{\rho})$ and circ $(\boldsymbol{\rho}_0 - 1/2\,\Delta\boldsymbol{\rho})$ in the $\boldsymbol{\rho}_0$ plane for an arbitrary $\Delta\boldsymbol{\rho}$. Notice that the area of overlap will always be centered at the origin of the $\boldsymbol{\rho}_0$ plane and that the area of overlap is dependent only on $|\Delta\boldsymbol{\rho}|$, and not on the location of $\Delta\boldsymbol{\rho}$ in the $\boldsymbol{\rho}_0$ plane. Furthermore, since the Gaussian function in $\boldsymbol{\rho}_0$ is circularly symmetric, the inner integral of Eq. (26), over the $\boldsymbol{\rho}_0$ plane, will also be independent of the angle of $\Delta\boldsymbol{\rho}$.

Since the inner integral of Eq. (26) does not depend on the direction of $\Delta\boldsymbol{\rho}$, it is convenient to choose $\Delta\boldsymbol{\rho}$ along either the $x$ or the $y$ axis in order to perform the integration. Choosing $\Delta\boldsymbol{\rho}$ along the $y$ axis and integrating yields

$$\begin{aligned} E[\tilde{P}_{\mathrm{sig}}] \approx 2T_0 P_{\mathrm{TX}} \left(\frac{d_R}{L}\right)^2 \sqrt{\pi} \int_0^1 \mathrm{d}u \, \exp\left[-\left(\frac{1}{2}R^2 + a^2\right)u\right] \\ \times \int_0^{a(1-u)^{1/2}} \exp(-x^2) \, \mathrm{erf}[(a^2 - x^2)^{1/2} - a\sqrt{u}] \, \mathrm{d}x , \end{aligned} \tag{29}$$

where $u$ is simply a dummy integration variable, and erf denotes the error function.[18] Finally, dividing the expected power propagating in the fiber by the expected power $E[\tilde{P}_{\mathrm{RX}}]$ collected by the receiver aperture results in an expression for the coupling efficiency for the single-mode fiber mixer. Specifically, the average expected power collected by the receiver aperture can be written as

$$E[\tilde{P}_{\mathrm{RX}}] = P_{\mathrm{TX}} T_0 \frac{A_R}{L^2} = P_{\mathrm{TX}} \frac{\tau}{\pi} \frac{\pi d_R^2}{4L^2} , \tag{30}$$

where $A_R$ is the area of the receiver aperture and $A_R/L^2$ is

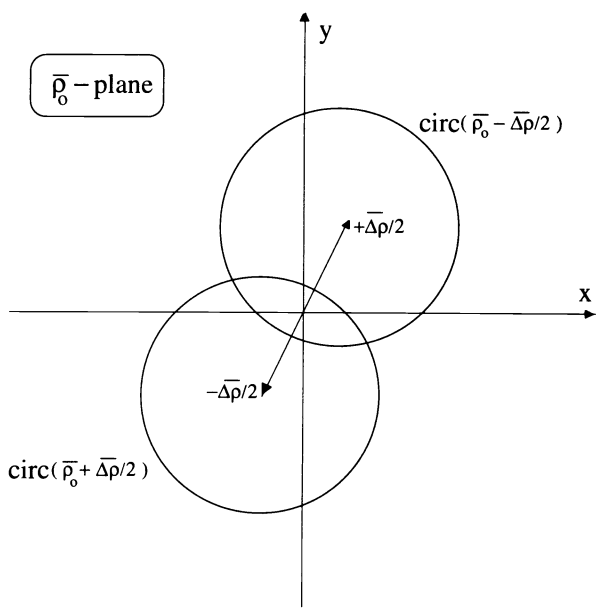


**Fig. 2** Circ-function overlap: The relationship between the two circ functions of Eq. (26) for an arbitrary displacement $\Delta\boldsymbol{\rho}$ in the $\boldsymbol{\rho}_0$ plane.

the solid angle subtended by the receiver aperture at the target. The expression for the coupling efficiency thus becomes

$$\eta_c = \frac{E[\tilde{P}_{\text{sig}}]}{E[\tilde{P}_{\text{RX}}]} \approx \frac{8}{\sqrt{\pi}} \int_0^1 du \exp\left[ -\left(\frac{1}{2}R^2 + a^2\right)u \right] \times \int_0^{a(1-u)^{1/2}} \exp(-x^2)\, \text{erf}[(a^2 - x^2)^{1/2} - a\sqrt{u}]\, dx \ . \tag{31}$$

Notice that for very distant targets the coupling efficiency, so expressed, is independent of the target range and for a given $a$ value depends solely on the truncation ratio $R = d_R/\omega_0$.

## 6 Optimizing the Coupling Efficiency

Figure 3 is a plot of coupling efficiency as a function of $a$ for four $R$ values: 4 (i.e., negligible truncation of the transmit beam[19]), 6, 8, and 10. Notice that the optimum coupling efficiency of 30.6% occurs at an $a$ value of 1.84 when $R = 4$. From Fig. 3 we also notice that as the truncation ratio increases, the coupling efficiency decreases. Qualitatively, the reason for this is easy to understand when one considers a constant transmit-receive aperture diameter and a decreasing transmit-beam waist. Namely, as the transmit-beam waist decreases, the beam pattern in the far field increases in size, thereby causing higher spatial frequencies at the receiver, which are less likely to couple into the single-mode fiber. Similarly, we expect systems that operate with truncation ratios less than 4 to experience lower coupling efficiencies due to increased diffraction of the transmitted beam.

Notice that for each $R$ value, the coupling efficiency is maximum for $a$ values approximately equal to 2. We can thus determine the relationship between the $f$ number (focal length divided by clear aperture diameter) of the receiver coupling optics and the numerical aperture of the single-mode fiber for optimum coupling. Recall that the parameter $a$ is given by

$$a \equiv \frac{1}{\sqrt{2}} \frac{\pi \omega d_R}{\lambda f} \ , \tag{32}$$

where $\omega$ is the optimum mode field diameter as a function of $V$ given by Eq. (23), $d_R$ is the receiver aperture diameter, and $f$ is the focal length of the coupling optics. From Eq. (23) we can also express the ratio $\omega/\lambda$ as

$$\frac{\omega}{\lambda} \equiv \frac{r_c}{\lambda} g_0(V) = V \cdot \frac{g_0(V)}{2\pi(\text{NA}_{\text{fiber}})} \ . \tag{33}$$

Substituting Eq. (33) into Eq. (32) yields

$$a = \frac{1}{2\sqrt{2}} \frac{V g_0(V)}{\text{NA}_{\text{fiber}}\ (f/\#)} = \frac{1}{\sqrt{2}} V g_0(V) \frac{\text{NA}_{\text{optics}}}{\text{NA}_{\text{fiber}}} \ , \tag{34}$$

or

$$a = C_a \frac{\text{NA}_{\text{optics}}}{\text{NA}_{\text{fiber}}} \ , \tag{35}$$

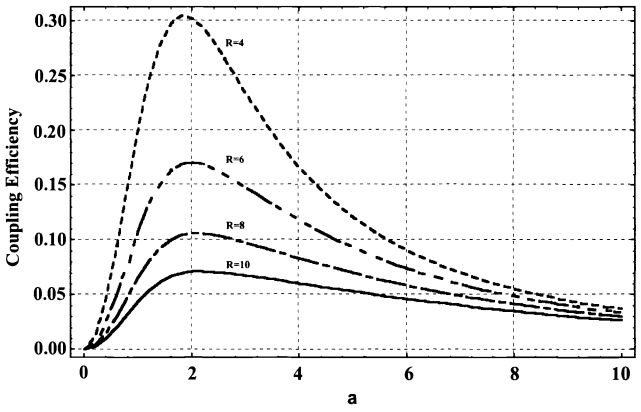


**Fig. 3** Single-mode fiber diffuse return coupling efficiency versus $a$ for four values of $R = d_R/\omega_0$: 4, 6, 8, and 10.

where $C_a$ is referred to as the $a$-parameter constant. Notice that $C_a$ depends solely on $V$; for single-mode fibers (i.e., $1.5 \leq V \leq 2.4$) it can be shown to vary from approximately 1.79 to 1.89. From Fig. 3 we also see that optimum coupling for each truncation ratio occurs for $a$ values approximately in the range 1.85 to 2.05. According to Fig. 3, the optimum coupling efficiency of 30.6% occurs for $R = 4$ at an $a$ value of 1.84. thus for single-mode fibers operating at approximately $V = 2.3$, optimum coupling occurs when the numerical apertures of the fiber and the coupling optics are matched. This is precisely the result we would have expected from a geometrical-optics point of view, thus validating our preceding analysis. Lastly, we would like to mention that through a more rigorous and numerically complex treatment incorporating the actual $LP_{01}$ modal solution for a weakly guiding single-mode optical fiber, we have determined an optimum coupling efficiency of 30.0% for $R = 4$, $V = 2.4$, and matched numerical apertures.

## 7 Summary

Real-world ladar systems commonly incorporate single-mode fiber mixers because of the robustness they introduce into the ladar systems. The performance of such a system, however, depends on how efficiently the received power couples into the fiber mixer. This paper has attempted to quantify this coupling efficiency for a system incorporating a single-mode fiber mixer while assuming a purely speckle target located in the far field.

We have shown that the coupling efficiency is maximized when the numerical aperture of the coupling optics is approximately matched to the numerical aperture of the single-mode fiber. We have also shown that the coupling efficiency is inversely related to the ladar-system truncation ratio. For a ladar system operating with negligible truncation of the transmit beam, the expected coupling efficiency is approximately 30%. Thus by simply replacing a free-space mixing arrangement with a single-mode fiber mixing arrangement in an untruncated system (i.e., $R = 4$), the system efficiency increases from 25% to 30%. Also, for a ladar system that is not operating with matched numerical apertures, the relations developed in Sec. 6 can be used for a particular truncation ratio to give a better prediction of the system performance.

### Acknowledgments

The authors would like to thank the Wright Laboratory Electro-Optic Sensor Group as well as the University of Dayton Center for Electro-Optics for providing research facilities, funding and technical support. This work has been sponsored by the Wright Laboratory Avionics Directorate and Technology/Scientific Services Inc. of Dayton Ohio, under contract F33601-95-DJ010.

### References

1. T. J. Kane, "Coherent laser radar at 1.06 microns using solid state lasers," PhD Dissertation, Univ. of Michigan (1986).
2. A. V. Jelalian, *Laser Radar Systems,* Artech House, Boston (1992).
3. A. Yariv, *Optical Electronics,* 3rd ed., Holt, Rinehart and Winston, New York (1985).
4. R. L. Schwiesow and R. F. Calfee, "Atmospheric refractive effects on coherent lidar performance at 10.6 μm," *Appl. Opt.* **18**(23), 3911–3917 (Dec. 1979).
5. C. G. Bachman, *Laser Radar Systems and Techniques,* Artech House, Boston (1979).
6. J. H. Shapiro, B. A. Capron, and R. C. Harney, "Image and target detection with a heterodyne reception optical radar," *Appl. Opt.* **20**(19), 3292–3313 (Oct. 1981).
7. R. M. Gagliardi and S. Karp, *Optical Communications,* Wiley, New York (1976).
8. M. B. Mark, "A comparison of free-space and fiber mixing performances," Wright Laboratories Technical Memo, Wright Patterson AFB, OH (Apr. 1992).
9. M. B. Mark, "A comparison of free space and fiber mixer performance in a heterodyne laser radar," in *Proc. IEEE 1992 National Aerospace and Electronics Conf. (NAECON),* Vol. 3, pp. 1256–1262 (1992).
10. B. J. Rye and R. G. Frehlich, "Optimal truncation and optical efficiency of an apertured coherent lidar focused on an incoherent backscatter target," *Appl. Opt.* **31**(15), 2891–2899 (May 1992).
11. G. Keiser, *Optical Fiber Communications,* McGraw-Hill, New York (1991).
12. J. T. Verdeyen, *Laser Electronics,* 2nd ed., Prentice-Hall, Englewood Cliffs, NJ (1989).
13. A. W. Snyder, "Excitation and scattering of modes on a dielectric or optical fiber," *IEEE Trans. Microwave Theory and Techniques* **MTT-17**(17), 1138–1144 (Dec. 1969).
14. J. H. Shapiro, "Target reflectivity theory for coherent laser radar," *Appl. Opt.* **12**(15), (Sept. 1982).
15. F. B. HildeBrand, *Advanced Calculus for Engineers,* Prentice-Hall, Englewood Cliffs, NJ (1949).
16. M. R. Spiegel, *Vector Analysis,* McGraw-Hill, New York (1959).
17. D. Marcuse, "Loss analysis of singlemode fiber splices," *Bell System Tech. J.* **56**(5), 703–718 (May–June 1977).
18. P. G. Hoel, *Introduction to Mathematical Statistics,* Wiley, New York (1984).
19. W. J. Smith, *Modern Optical Engineering,* McGraw-Hill, New York (1986).

**Donald K. Jacob** received his Bachelor of Science degree in photonics from the State University of New York Utica/Rome in 1991. In 1994 he received his Master of Science degree in electro-optics from the University of Dayton. His research interests include fiber optics and integrated optics.

**Martin B. Mark:** Biography and photograph appear with the paper "Analysis of ladar range resolution enhancement by sinusoidal phase modulation" in this issue.

**Bradley D. Duncan:** Biography and photograph appear with the special section guest editorial in this issue.